Science of the Total Environment 870 (2023) 161931

Contents lists available at ScienceDirect

Science of the Total Environment

journal homepage: www.elsevier.com/locate/scitotenv

Plant-minerals-water interactions: An investigation on *Juncus acutus* exposed to different Zn sources

Daniela Medas [a,*], Carlo Meneghini [b], Claudia Pusceddu [a], Ilaria Carlomagno [c], Giuliana Aquilanti [c], Elisabetta Dore [a], Vittorio Murgia [d], Francesca Podda [a], Valentina Rimondi [e,f], Salvatore Vacca [a], Richard B. Wanty [g], Giovanni De Giudici [a]

[a] Department of Chemical and Geological Science, University of Cagliari, Cagliari, Italy
[b] Department of Sciences, University of Roma Tre, Rome, Italy
[c] Elettra-Sincrotrone Trieste, Basovizza, Trieste, Italy
[d] Soc. Agr. Sgaravatti Land Cons. Arl, Cagliari, Italy
[e] Department of Earth Sciences, University of Florence, Florence, Italy
[f] CNR—Institute of Geosciences and Earth Resources, Florence, Italy
[g] Colorado School of Mines, Department of Geology and Geological Engineering, Golden, CO 80401, USA

HIGHLIGHTS

- Zn tolerance occurs by Zn complexation to citrate and cysteine.
- Variation of Zn content in water lead to different uptake mechanisms.
- Zn complexation by *J. acutus* is mainly influenced by rhizosphere mineralogy.

GRAPHICAL ABSTRACT

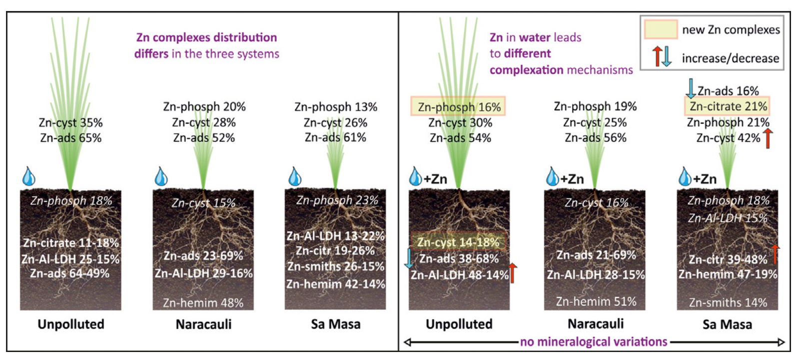

ARTICLE INFO

Editor: Filip M.G. Tack

Keywords:
Pollutants
Metal speciation
Rhizosphere minerals
XANES

ABSTRACT

Juncus acutus has been proposed as a suitable species for the design of phytoremediation plans. This research aimed to investigate the role played by rhizosphere minerals and water composition on Zn transformations and dynamics in the rhizosphere-plant system of *J. acutus* exposed to different Zn sources. Rhizobox experiments were conducted using three different growing substrates (Zn from 137 to 20,400 mg/kg), and two irrigation lines (Zn 0.05 and 180 mg/l). The plant growth was affected by the substrate type, whereas the Zn content in the water did not significantly influence the plant height for a specific substrate. *J. acutus* accumulated Zn mainly in roots (up to 10,000 mg/kg dw); the metal supply by the water led to variable increases in the total Zn concentration in the vegetal organs, and different Zn distributions both controlled by the rhizosphere mineral composition. Different Zn complexation mechanisms were observed, mainly driven by cysteine and citrate compounds, whose amount increased linearly with Zn content in water, but differently for each of the investigated systems.
Our study contributes to gain a more complete picture of the Zn pathway in the rhizosphere-plant system of *J. acutus*. We demonstrated that this vegetal species is not only capable of developing site-specific tolerance mechanisms, but it is

* Corresponding author.
E-mail addresses: dmedas@unica.it (D. Medas), carlo.meneghini@uniroma3.it (C. Meneghini), ilaria.carlomagno@elettra.eu (I. Carlomagno), giuliana.aquilanti@elettra.eu (G. Aquilanti), elisabetta.dore@unica.it (E. Dore), vittorio.murgia@sgaravattigroup.it (V. Murgia), fpodda@unica.it (F. Podda), valentina.rimondi@unifi.it (V. Rimondi), salvacca@unica.it (S. Vacca), rwanty@mines.edu (R.B. Wanty), gbgiudic@unica.it (G. De Giudici).

http://dx.doi.org/10.1016/j.scitotenv.2023.161931
Received 17 October 2022; Received in revised form 27 January 2023; Accepted 27 January 2023
Available online 31 January 2023

also capable to differently modulate Zn transformation when Zn is additionally supplied by watering. These findings are necessary for predicting the fate of Zn during phytoremediation of sites characterized by specific mineralogical properties and subject to water chemical variations.

1. Introduction

Trace metals occur naturally in rocks, soils and waters, but higher quantities are being released into the environment by anthropogenic activities (Kwon et al., 2022; Zovko and Romic, 2011), such as industrial, mining, shipping and agricultural ones. As a result, there is a strong need for efficient tools to prevent metal dispersion (Wang et al., 2021; Zhou et al., 2020; Zoumis et al., 2000) and transfer to the food chain. Phytostabilization is an especially suitable method in highly polluted areas (Frérot et al., 2006; Pérez-Esteban et al., 2014; Salt et al., 1995). It exploits plant cover to prevent pollutants from spreading by erosion, water infiltration, leaching and from toxic dust dispersal by wind (Frérot et al., 2006, and references therein). *Juncus acutus* L. is a plant species characterized by i) a sub-cosmopolitan distribution, ii) a wide ecological range, iii) a high dispersion potential, due to its abundant seed production and high germination rate, and iv) a great tolerance to high concentration of metals, sulphates and chlorides, and to hydric stress during the dry summer season (Brown and Bettink, 2006; Fancello et al., 2019; Freitas et al., 2009; Landsberger et al., 2010; Lombardo, 1982; López-Juambeltz et al., 2020; Mateos-Naranjo et al., 2018, 2014; Santos et al., 2014; Stefani et al., 1991; Syranidou et al., 2017a). These properties make *J. acutus* and its interactions with the environment of great relevance for a multidisciplinary and global audience. As for other macrophytes (Marchand et al., 2010), *J. acutus* plays a significant role in the riverbed processes, reducing metal mobility by limiting erosive processes, promoting the sedimentation of suspended particles, providing organic matter for bacterial metabolism, and potential sites for metal sorption. It was also observed that *J. acutus* can favor the formation of authigenic sulfides (mainly FeS_2) in the hyporheic zone (Dore et al., 2020). These features make this plant species an effective phytostabilizer, useful for revegetation of Zn-contaminated lands (Mateos-Naranjo et al., 2014; Syranidou et al., 2017a), and as a tool for wetland restoration projects around the world (Aydın Temel et al., 2018; Santos et al., 2014; Sparks et al., 2013; Zaimoglu, 2006).

Understanding the interactions between metals and plants is a fundamental issue because metals released into the environment will inevitably interact with plants, which are basic components of ecosystems. Moreover, revealing metal mobilization/immobilization processes at the molecular level is fundamental to develop effective phytoremediation strategies. Several experimental investigations were conducted on *J. acutus* grown under different Zn concentrations (Mateos-Naranjo et al., 2018, 2014; Santos et al., 2014), and the increasing number of literature studies (Alam et al., 2022; Christofilopoulos et al., 2016; Duarte et al., 2021; Syranidou et al., 2017b, 2017a, 2016) demonstrates the interest and the need for an in-depth knowledge of metal geo-biotransformation in the rhizosphere-plant system of *J. acutus*. To the best of our knowledge, previous researches specifically aimed at investigating the relationship between Zn source and Zn complexation in plants (da Cruz et al., 2019; Doolette et al., 2018; Montanha et al., 2020; Wang et al., 2013) are limited and need further investigations. Our work delves into the understanding of Zn transformations and dynamics during rhizosphere-plant interactions when plants are exposed to different metal sources. Previous studies (Medas et al., 2019) demonstrated that *J. acutus* grown in natural mining environments can optimize its adaptation in response to the mineralogy and geochemical conditions of the site. In the present paper, a rhizobox experiment (Hylander, 2002) was set up, under greenhouse conditions, to isolate the influence of rhizosphere minerals and water composition. Three different growing substrates (two polluted substrates from abandoned mining sites and an unpolluted potting soil) and two different irrigation lines (Clean Water Line – Zn_{water} 0.05 mg/l; Zn-spiked Water Line – Zn_{water} 180 mg/l) were employed. A multi-technique characterization, combining chemical, X-ray diffraction (XRD) and X-ray absorption near edge structure (XANES) analyses to investigate Zn distribution and complexation, was employed. The aim was to reach a better understanding of the Zn pathway in the rhizosphere-plant system, and to assess the role played by the rhizosphere minerals and water composition on Zn uptake processes.

2. Materials and methods

2.1. Rhizobox experiment

Rhizobox experiment was performed in the greenhouse “Vivai Murgia” (Villacidro, SW Sardinia). The rhizoboxes (Fig. 1) were made up of transparent plexiglass (L × H × W = 200 × 300 × 50 mm) and were laterally covered by removable strips of dark fabric to protect the roots from light. Eighteen rhizoboxes were divided into two groups and were placed onto two wooden supports. The rhizoboxes were filled by three different substrates (three replicates for each substrate): i) two different muddy mine wastes, one from the Naracauli area (N39° 31.14′, E8° 29.33′, Naracauli substrate; Medas et al., 2013) and one from the San Giorgio area (N39° 16.56′, E8° 27.39′, Sa Masa substrate; Bacchetta et al., 2015; De Giudici et al., 2017) (SW Sardinia); ii) an unpolluted substrate (potting soil) (see Table S1 for Zn, Pb, Cd, C_{tot}, N_{tot} and H_{tot} contents, and pH values). The substrates were sieved at 2 mm, and 2 kg of each substrate were mixed with 1 kg of commercial pozzolana, to improve their permeability. After mixing, each rhizobox was filled with the mixture.

To increase the chances for the plants to grow in the substrates characterized by high metal concentrations (Kothe and Büchel, 2014; Sprocati et al., 2014), plantlets of *J. acutus* were obtained from seeds collected from plants growing in the Naracauli mine-polluted area (Sprocati et al., 2014). The plantlets were grown up to 5–10 cm in potting soil (Fig. 1a), then their roots were gently cleaned from particles of the initial substrate, and plants were transferred in the rhizoboxes (Fig. 1b, and c). Two plantlets were transplanted in each rhizobox.

Two irrigation lines were used, one with unpolluted water (Clean Water Line, *i.e.*, tap water, average Zn_{water} 0.05 mg/l, hereinafter referred to as CW), and another with polluted water (Zn-spiked Water Line, Zn_{water} 180 mg/l, hereinafter referred to as ZnW) (Fig. 1c and d). Watering was provided every 48 h according to the seasonal conditions (max temperatures up to 45 °C in August). Zinc was supplied to the ZnW as $ZnSO_4{\cdot}7H_2O$. This choice is justified by the fact that many mine-affected waters in the Sardinia districts have Zn and SO_4 as major ions (Cidu et al., 2011; De Giudici et al., 2019; Medas et al., 2012). Moreover, the specific Zn concentration selected is within the range reported for mine waste pore water, seepages and river waters draining several abandoned or active mining areas around the world (Bao et al., 2022; Cidu and Biddau, 2005; Pavoni et al., 2018).

The experiment lasted five months, and the growth of plants was monitored monthly, measuring *J. acutus* height from the surface of the substrate to the highest part of the plant. At the end of the experiment, plants and rhizospheres (defined here as the soil portion collected within 2 mm from the roots) were collected and analyzed. All triplicates, both the vegetal organs and the rhizospheres, were mixed to have enough material to perform XRD, Zn chemical analysis and XANES investigation. Table S2 shows the investigated sample names and their description.

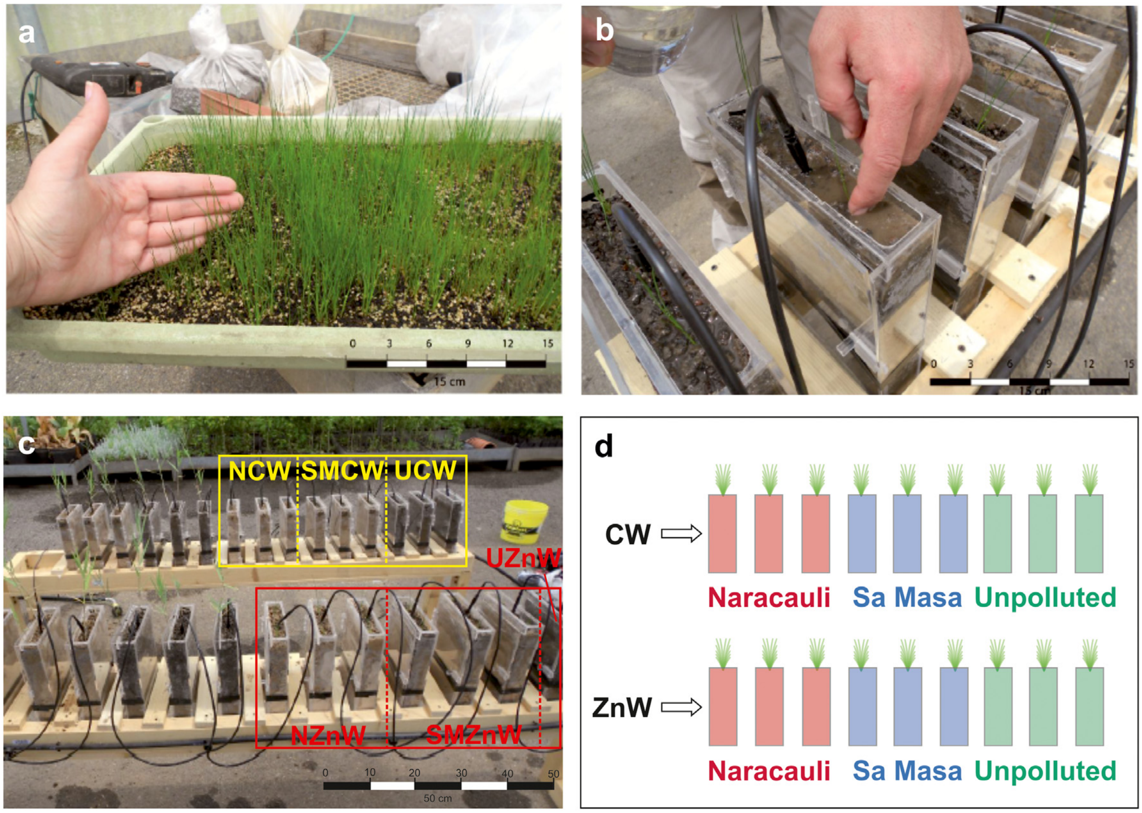

Fig. 1. (a) Plantlet of *J. acutus* before the rhizobox experiment; (b) transplantation into the rhizoboxes (the black tubes are irrigation lines); (c) overview of the rhizoboxes (still uncovered by dark fabric); (d) scheme of the rhizobox experiment. The yellow and red rectangles in 1c indicate the rhizoboxes with *J. acutus*. UCW (Unpolluted substrate Clean Water Line), NCW (Naracauli, substrate Clean Water Line), SMCW (Sa Masa substrate Clean Water Line), UZnW (Unpolluted substrate Zn-spiked Water Line), NCW (Naracauli, substrate Zn-spiked Water Line), SMCW (Sa Masa substrate Zn-spiked Water Line).

2.2. X-ray diffraction and chemical analysis

XRD analysis was performed on the substrates (before the rhizobox experiment), rhizospheres (after the rhizobox experiment), and on the vegetal organs (roots and stems, after the rhizobox experiment) by a laboratory θ–θ equipment (Panalytical X'Pert Pro, Almelo, Netherlands) operating at 40 kV and 40 mA with Ni-filtered Cu K_α radiation (λ = 1.54060 Å), using the X'Celerator detector. Diffraction patterns were analyzed with X'Pert HighScore Plus 2.1 (Panalytical, Almelo, The Netherlands) using the PDF-2 database (International Centre for Diffraction Data) to identify the crystallographic phases in the samples (see section S1 of the Supplementary Material for more details on XRD analysis).

For Zn determination in the solid samples (substrates, rhizospheres and vegetal organs), acid digestion was carried out. Samples were processed together with blanks and selected reference materials (NIST 2710, Montana Soil for the substrates and rhizospheres; SRM 1573a, tomato leaves for the vegetal organs), prepared with the same procedure, to evaluate the precision (<5 %) and accuracy (<5 %) of the digestion procedure. Then, Zn was determined by inductively coupled plasma optical emission spectrometry (ICP-OES, ARL Fisons ICP Analyzer 3520 B, Waltham, MA, USA). To estimate potential contaminations, the accuracy (<5 %) and precision (<5 %) of trace element analysis, procedural blanks and reference solutions (SRM 1643e and EnviroMAT Drinking Water, High EP-H-3 and Low EP-L-3) were analyzed together with the samples (see section S2 of the Supplementary Material for more details on chemical analysis).

Zinc uptake by plants was evaluated by three different factors: the biological concentration factor (BCF), the bioaccumulation coefficient (BAC), and the translocation factor (TF). The BCF quantifies the Zn (mg/kg) transfer from the rhizosphere (M_{rhizo}) to the roots (M_{roots}) (Fellet et al., 2007) according to Eq. (1):

$$BCF = \frac{M_{roots}}{M_{rhizo}} \quad (1)$$

The BAC (Eq. (2)) estimates the transfer of Zn (mg/kg) from the rhizosphere (M_{rhizo}) to the epigean organs (M_{epi}) (Marchiol et al., 2013):

$$BAC = \frac{M_{epi}}{M_{rhizo}} \quad (2)$$

The TF (Eq. (3)) evaluates the translocation of Zn (mg/kg) from the roots (M_{roots}) to the epigean organs (M_{epi}) (Brooks, 2008):

$$TF = \frac{M_{epi}}{M_{roots}} \quad (3)$$

Determination of pH was performed for the substrate samples according to the procedures published by Food and Agriculture Organization of the United Nations (FAO, 2021) (soil to water ratio 1:2.5 *w/v*). Total C (C_{tot}), N (N_{tot}), and H (H_{tot}) contents in substrates were determined by using an elemental analyzer (CHN-1000, LECO Corporation, MI, USA). The sample was placed in a tin capsule and inserted in the furnace at 1000 °C in excess of oxygen, then the products of combustion were passed into a second furnace at 850 °C. The gases were collected and homogenized in the ballast, then sent to detectors. Samples were processed together with a reference material (Orchard Leaves, Nist SRM 2691). Results are reported in Table S1.

2.3. X-ray absorption spectroscopy

Synchrotron-based techniques, such as XANES spectroscopy, are being employed increasingly in the investigation of soil-plant systems, and represent a suitable and powerful tool for unravelling the chemical speciation of metals and metalloids (Adediran et al., 2015; Chandrakasan et al., 2021; Chen et al., 2022; De Giudici et al., 2015; Fourati et al., 2020; Kopittke et al., 2017; Panfili et al., 2005; Parsons et al., 2002; Saraswat and Rai, 2011; Sarret et al., 2013; Zelano et al., 2020; Zhao et al., 2014). Zinc K-edge (9.659 keV) XANES measurements were performed at the XAFS beamline (Di Cicco et al., 2009) (experiment #20167045), and at the XRF beamline (Jark et al., 2014) at Elettra-Sincrotrone Trieste, Italy.

Since in the soil-plant system Zn can be hosted in mineral phases (*e.g.*, sulfides, sulphates, carbonates, *etc.*) and/or can be bound to organic compounds (*e.g.*, organic acids, phytochelatins, metallothioneins, *etc.*) (Caldelas and Weiss, 2017; de la Fuente et al., 2018; Kopittke et al., 2017; Parsons et al., 2002; Salt et al., 1999; Saraswat and Rai, 2011; Sarret et al., 2006, 2002; Zhao et al., 2014), a large set of Zn reference compounds (standards, Table S3) was measured or derived from previous experiments (Boi et al., 2020; Medas et al., 2018) carried out with the same set-up. The measurements of the reference compounds allowed us to reliably compare the datasets collected on the two beamlines. Athena software (Ravel and Newville, 2005) was used for preliminary XAS data treatment (background subtraction, normalization and averaging) and quantitative XANES analysis (linear combination analysis, LCA). The normalized XANES spectra of the reference compounds are shown in Fig. S1.

The principal component analysis (PCA) was performed by the SixPack software (Webb, 2005) to evaluate the number of statistically significant components (principal components) necessary to describe the variability of the experimental signals within the dataset (Etschmann et al., 2014). The target transform (TT) was used to select, among the reference compounds, the most suitable to be used to reproduce (LCA) the sample experimental data (Gaur and Shrivastava, 2012; Shi et al., 2008; Voegelin et al., 2005; Wang et al., 2013). Normalized sample spectra where then analyzed by LCA by Athena software (Ravel and Newville, 2005), within an energy range of −20 eV below to +30 eV above the edge, selecting the suitable references identified by TT. For each sample, the combination of standards with the lowest R-factor and the lowest reduced χ^2 was selected as the most likely set of components (see section S3 of the Supplementary Material for more details on XAS data analysis).

3. Results

3.1. Plant growth, substrate and rhizosphere characterization

Heights of *J. acutus* seedlings were measured monthly during the experiment and their values are reported in Table 1 and Fig. S2. Plant height was similar in all systems through the first month, but by the end of the experiment, plants from the unpolluted substrate were higher, for both the CW (29 ± 5 cm after 5 months) and the ZnW (26 ± 1 cm after 5 months), than plants from the polluted substrates (Sa Masa: CW 17.3 ± 0.9 cm, ZnW 15 ± 1 cm; Naracauli: CW 12 ± 1 cm, ZnW 11.8 ± 0.7 cm).

Results of XRD analysis are reported in Table S4. Rhizospheres (from both the CW and ZnW) did not show any variation in mineralogical composition when compared to the corresponding initial substrate. Quartz (SiO_2) and calcite ($CaCO_3$) were detected in all the substrates and rhizospheres. Accessory minerals were siderite ($FeCO_3$) and gypsum ($CaSO_4$) in the Naracauli samples, while smithsonite ($ZnCO_3$) and hemimorphite ($Zn_4Si_2O_7(OH)_2{\cdot}H_2O$) were observed in Sa Masa samples. The main peaks of quartz were also observed in all the roots. In all roots and stems, we clearly observed the main peaks of cellulose at around 14.9°–16.5° 2θ and 22.8° 2θ.

Initial substrates were characterized by slightly alkaline pH values (7.6–7.8). Low contents of N_{tot} (Sa Masa <DL, Naracauli 0.26 %) and H_{tot} (Sa Masa 0.23 %, Naracauli 0.43 %) were observed for both the mine substrates, coherently with their origin. Total C (C_{tot}) increased in the order Naracauli (1.16 %), unpolluted (3.04 %), and Sa Masa (8.95 %) substrate. It is worth noting that Sa Masa substrate was characterized by high amount of carbonate minerals (mainly calcite and dolomite, Table S4) and, consequently, a significant portion of C_{tot} was in the inorganic form according to Bacchetta et al., 2015 that reported 8.20 % of C_{tot} and 1.98 % of organic C (C_{org}) for samples collected in the same area.

3.2. Zinc concentration and distribution

Table 2 and Fig. S3 show the Zn concentrations in the investigated samples. At the beginning of the experiment, the substrates were characterized by different Zn concentrations in the order: unpolluted (Zn 137 ± 4 mg/kg), Naracauli (Zn 9700 ± 291 mg/kg) and Sa Masa (Zn 20,400 ± 612 mg/kg). As for the substrates, Zn increased from the unpolluted rhizospheres (Zn 150–3040 mg/kg) to the Naracauli (Zn 10,400–12,500 mg/kg) and Sa Masa (Zn 19,500–20,600 mg/kg) rhizospheres both in samples from the CW and the ZnW. Zinc contents in *J. acutus* roots and stems were affected by the Zn concentrations in the rhizospheres (correlation coefficient

Table 1

Plant growth during the experiment in the different substrates and irrigation lines. The uncertainty was calculated as $\frac{\text{standard deviation(height measurements)}}{\sqrt{\text{number of measurements}}}$, where n is the number of measurements ($n = 6$, two plants for each rhizobox in triplicate).

		1 month	2 months	3 months	4 months	5 months
		Height (cm)	Height (cm)	Height (cm)	Height (cm)	Height (cm)
Clean Water Line (Zn_{water} 0.05 mg/l)						
Unpolluted	Mean	7.8	20.4	23	27	29
	Uncertainty	0.6	0.8	1	2	5
Naracauli	Mean	6.9	10	10.9	11.2	12
	Uncertainty	0.7	1	0.8	0.9	1
Sa Masa	Mean	6.8	12.8	14	16.3	17.3
	Uncertainty	0.7	0.3	1	0.9	0.9
Zn-spiked Water Line (Zn_{water} 180 mg/l)						
Unpolluted	Mean	7.8	20	23	24	26
	Uncertainty	0.6	2	2	2	1
Naracauli	Mean	7.2	10.4	11.4	11.7	11.8
	Uncertainty	0.2	0.7	0.6	0.6	0.7
Sa Masa	Mean	7.1	11	12	13	15
	Uncertainty	0.9	1	1	1	1

Table 2
Zinc content in the substrates, rhizospheres, roots and stems of *J. acutus* from the Clean Water Line and the Zn-spiked Water Line.

		Before the rhizobox experiment	Before the rhizobox experiment
		Zn (mg/kg)	Zn (mg/kg)
Substrates	Unpolluted	137 ± 4	137 ± 4
	Naracauli	9700 ± 291	9700 ± 291
	Sa Masa	20,400 ± 612	20,400 ± 612
		Clean Water Line (Zn_{water} 0.05 mg/l)	Zn-spiked Water Line (Zn_{water} 180 mg/l)
		Zn (mg/kg)	Zn (mg/kg)
Rhizospheres	Unpolluted	150 ± 5*	3040 ± 91*
	Naracauli	10,400 ± 312*	12,500 ± 375*
	Sa Masa	19,500 ± 585	20,600 ± 618
Roots	Unpolluted	59 ± 2*	123 ± 4*
	Naracauli	4400 ± 132	4700 ± 141
	Sa Masa	5900 ± 177*	10,000 ± 300*
Stems	Unpolluted	41 ± 1*	62 ± 2*
	Naracauli	420 ± 13*	480 ± 14*
	Sa Masa	870 ± 26*	1140 ± 34*

* p-Value < 0.01.

$\rho_{Zn\text{-}rhizo\text{-}roots}$ 0.94–0.99, $\rho_{Zn\text{-}rhizo\text{-}stems}$ 0.97–0.99), and followed the same trend (Zn concentration in Sa Masa *J. acutus* > Naracauli > unpolluted) along the two irrigation lines (Table 2 and Fig. S3).

We observed significant statistical differences (*Z*-test, *p*-value < 0.01) between the Zn concentrations in samples from the two irrigation lines in all the investigated systems, except for the Sa Masa rhizosphere and Naracauli roots in which the Zn concentration changes were weaker (p-value > 0.1). The rhizosphere, roots and stems from the unpolluted group showed the highest increase in Zn concentration (1930 % in the rhizosphere, 108 % in the roots, and 51 % in the stems) when plants were watered with the Zn-spiked water. In the Sa Masa group, the rhizosphere did not show any statistically significant Zn increase, whereas in roots and stems the metal concentration increased by 69 % and 31 %, respectively. For the Naracauli group, Zn increased by 20 % in the rhizosphere and by 14 % in the stems, while in the roots the difference was weak and not statistically significant.

Variations were also observed for the Zn accumulation and distribution as described by the indexes reported in Table 3 and Fig. S4 (BCF, Zn_{roots}/Zn_{rhizo}; BAC, Zn_{epi}/Zn_{rhizo}; TF, Zn_{epi}/Zn_{roots}). In the samples from the CW, BCF values were similar for the three systems (BCF 0.30–0.42), whereas BAC and TF were higher for the plants grown on the unpolluted substrate (BAC 0.24, TF 0.69) than for plants grown on the contaminated substrates (BAC 0.04, TF 0.10–0.15), indicating that Zn accumulation in stems and its translocation were higher when Zn content in the rhizosphere was low (150 mg/kg). For the ZnW samples, indexes for the plants grown on the unpolluted substrate showed the most important variations, and they decreased (Table 3), pointing out a lower Zn uptake and translocation than *J. acutus* plants from the CW. Specifically, the BCF for the unpolluted group reached the lowest value in comparison to the contaminated systems,

Table 3
BCF (biological concentration factor), BAC (bioaccumulation coefficient) and TF (translocation factor) calculated for *J. acutus* plants.

	BCF	BAC	TF
Clean Water Line (Zn_{water} 0.05 mg/l)			
Unpolluted	0.35	0.24	0.69
Naracauli	0.42	0.04	0.10
Sa Masa	0.30	0.04	0.15
Zn-spiked Water Line (Zn_{water} 180 mg/l)			
Unpolluted	0.04	0.02	0.50
Naracauli	0.38	0.04	0.10
Sa Masa	0.49	0.06	0.11

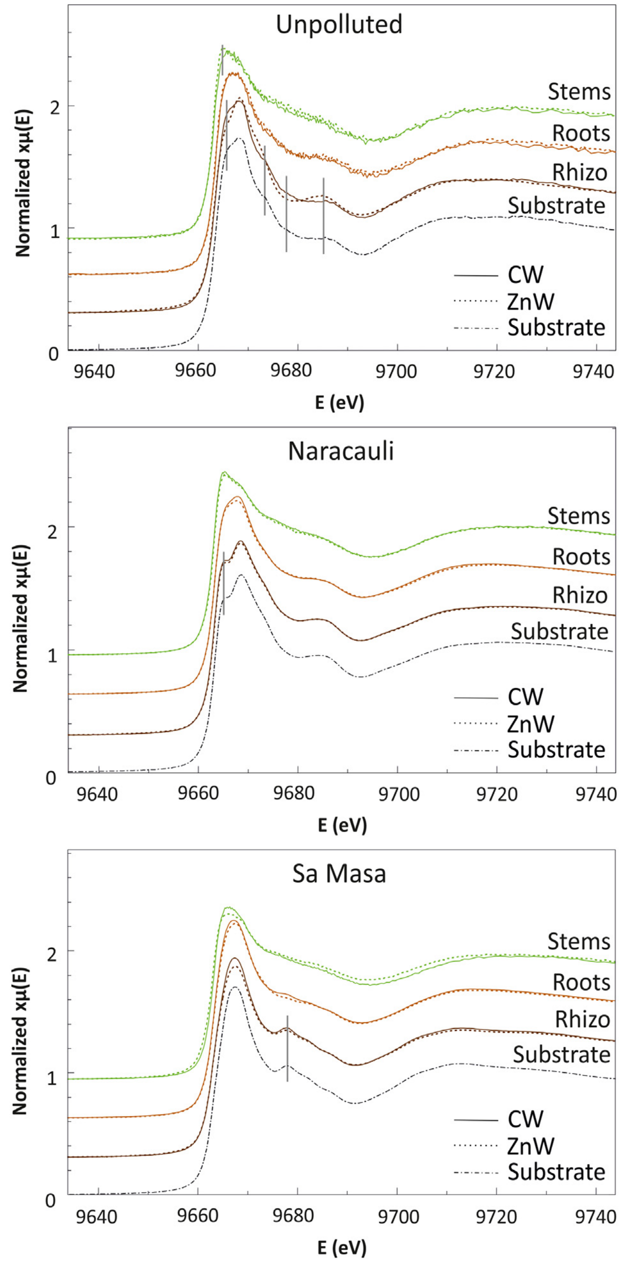

Fig. 2. Zn K-edge (9.659 keV) XANES spectra of the substrates, rhizospheres and vegetal organs (roots and stems) for the Clean Water Line (Zn_{water} 0.05 mg/l) and the Zn-spiked Water Line (Zn_{water} 180 mg/l), vertically shift for sake of comparison.

whereas the Zn translocation was the highest (TF 0.50), as for the CW. For the Sa Masa system, the BCF increased and showed the highest value (BCF 0.49), because of a higher Zn accumulation in roots in comparison to the other systems. On the contrary, BCF showed an inverse trend for the Naracauli group, slightly decreasing (BCF from 0.42 to 0.38). BAC and TF values for plants grown on both mine-waste-rich substrates did not depend on the Zn concentration of the irrigation water.

3.3. Zinc chemical speciation in solid samples

Molecular species of Zn in the initial substrates, rhizospheres and plant organs from the two irrigation lines were investigated by bulk XANES analysis (Fig. 2). XANES spectral features were more structured in the substrates and rhizospheres and became smoother and broader in the roots and stems. These characteristics suggested that the local structure around Zn was more disordered in the vegetal organs than in the substrates and rhizospheres.

The Zn K-edge XANES measured on the substrates and rhizosphere samples from the unpolluted and Naracauli systems depicted a double peak white line around 9665 eV, more pronounced in the Naracauli samples. The Zn-edge XANES of the Sa Masa substrate and rhizosphere showed a single peak white line and a broad shoulder in the post-edge region (9680 eV), definitely different from the spectra measured in unpolluted and Naracauli samples. However, the XANES features of the roots and stem samples appeared to preserve some of the Zn chemical species from the original substrates in all the experimental conditions.

To investigate the distribution of the Zn chemical species, we performed a PCA and a LCA using the spectra measured on standard Zn compounds (Table S3 and Fig. S1) as references (see Section S4, Tables S5 and S6, Fig. S5 for details on XANES data processing for PCA and LCA). LCA allowed us to identify seven different coordination environments: i) octahedral Zn (ZnO_6) in smithsonite, ii) octahedral Zn (ZnO_6) in layered double hydroxides (Zn-Al-LDH), iii) tetrahedral Zn (ZnO_4) in hemimorphite, iv) tetrahedral Zn (ZnO_4) in Zn phosphate, v) sorbed tetrahedral Zn on hydroxyapatite, vi) tetrahedral Zn (ZnS_4) in Zn cysteine, and vii) octahedral Zn (ZnO_6) complexed to citrate (Table 4 and Fig. S6a–h).

In all the substrates (Table 4), Zn was present as octahedral Zn (ZnO_6) in layered minerals (Zn-Al-LDH, 14–34 %). Sorbed tetrahedral Zn was detected in the unpolluted and Naracauli substrates, with the highest content in the unpolluted sample (62 %). In the Sa Masa substrate, relevant concentrations of tetrahedral Zn in hemimorphite (33 %) and octahedral Zn in smithsonite (29 %) were found, in agreement with XRD analysis (Table S4). Tetrahedrally coordinated Zn in hemimorphite was also detected in the Naracauli substrate (47 %). In this sample crystalline hemimorphite was not revealed by XRD, but it could be present below the detection limit of 1 % by volume, as hemimorphite is a typical ore mineral in the abandoned mine of Naracauli (Boni et al., 2003). Moreover, a local hemimorphite-like Zn coordination could be present as an amorphous phase. A portion of Zn was also found to be octahedrally bound to citrate in the unpolluted and Sa Masa samples. LCA results explained the differences observed between the XANES spectral features of unpolluted/Naracauli and Sa Masa samples. Indeed, the broad shoulder in the post-edge region (9680 eV) of the Sa Masa substrate was due to the presence of smithsonite, whereas the double peak white line around 9665 eV originated from the contribution of sorbed tetrahedral Zn and Zn-Al-LDH in the unpolluted sample, and from hemimorphite and Zn-Al-LDH in the Naracauli substrate (Fig. S7).

In the samples from the CW, Zn chemical speciation of the rhizospheres did not change significantly in comparison to the initial substrates (Table 4, Figs. S6c, S8–S10). In all roots (Table 4, Figs. S6b, S8–10), a fraction of Zn contribution (14–22 %) appeared to originate from residues of the rhizospheres (layered minerals, hemimorphite and smithsonite), supporting the qualitative XANES analysis (Fig. 2). In unpolluted-CW-roots and Naracauli-CW-roots, a high fraction (49–69 %) of Zn was present in a disordered environment, like sorbed tetrahedral Zn. In unpolluted-CW-roots and Sa Masa-CW-roots, we detected Zn bound to phosphate (18–23 %) and to citrate (18–26 %). A small portion (15 %) of Zn was complexed to cysteine in Naracauli-CW-roots. All the stems showed a similar Zn speciation, mainly sorbed Zn (up to 65 %) and Zn cysteine (up to 35 %). Zinc phosphate (13–20 %) was detected in Naracauli-CW-stems and Sa Masa-CW-stems.

For the ZnW samples (Table 4, Fig. S6e, f and g), differences in the Zn chemical speciation were found, and they were different in the three systems, as observed for the Zn accumulation (Table 2 and Fig. S3) and distribution (Table 3 and Fig. S4). In the unpolluted-ZnW-rhizo, we observed an increase in Zn-Al-LDH (from 25 to 48 %), a decrease in sorbed Zn (from 64 % to 38 %), and a contribution from Zn cysteine (14 %), compound not found in unpolluted-CW-rhizo. Differently from samples belonging to the CW, Zn cysteine (18 %) was observed in unpolluted-ZnW-roots, and Zn phosphate (16 %) in unpolluted-ZnW-stems. In the Sa Masa rhizosphere and roots, Zn citrate increased from 19 % (Sa Masa-CW-rhizo) to 39 % (Sa Masa-ZnW-rhizo), and from 26 % (Sa Masa-CW-roots) to 48 % (Sa Masa-ZnW-roots), respectively. In the Sa Masa stems, the sorbed Zn decreased from 61 % (Sa Masa-CW-stems) to 16 % (Sa Masa-ZnW-stems), while Zn cysteine increased from 26 % (Sa Masa-CW-stems) to 42 % (Sa Masa-ZnW-stems), and a portion of Zn (21 %) was bound to citrate in Sa Masa-ZnW-stems. For the Naracauli samples (rhizosphere, roots and stems), we did not find significant differences in the Zn chemical speciation in the samples from the two irrigation lines.

Table 4
Results from the linear combination analysis of XANES for the substrates, rhizospheres and vegetal organs (roots and stems) for the CW (Zn_{water} 0.05 mg/l) and the ZnW (Zn_{water} 180 mg/l). The sum of contribute fractions was fixed to 100 %, the uncertainty on the fraction values is around 8 %. *Ardau et al. (2012); Frau et al. (2020).

		Zn-Al-LDH* (%)	Hemimorphite (%)	Smithsonite (%)	Zn phosphate (%)	Zn in hydroxyapatite (%)	Zn citrate (%)	Zn cysteine (%)	R-factor ($\times 10^3$)	reduced χ^2 ($\times 10^3$)
Before the rhizobox experiment										
Substrates	Unpolluted	27	–	–	–	62	11	–	0.7	0.6
	Naracauli	34	47	–	–	19	–	–	0.3	0.2
	Sa Masa	14	33	29	–	–	24	–	0.1	0.09
Clean Water Line (Zn_{water} 0.05 mg/l)										
Rhizospheres	Unpolluted	25	–	–	–	64	11	–	0.7	0.6
	Naracauli	29	48	–	–	23	–	–	0.4	0.3
	Sa Masa	13	42	26	–	–	19	–	0.8	0.7
Roots	Unpolluted	15	–	–	18	49	18	–	0.4	0.3
	Naracauli	16	–	–	–	69	–	15	0.2	0.1
	Sa Masa	22	14	15	23	–	26	–	0.2	0.2
Stems	Unpolluted	–	–	–	–	65	–	35	0.5	0.4
	Naracauli	–	–	–	20	52	–	28	0.3	0.2
	Sa Masa	–	–	–	13	61	–	26	0.1	0.1
Zn-spiked Water Line (Zn_{water} 180 mg/l)										
Rhizospheres	Unpolluted	48	–	–	–	38	–	14	0.3	0.2
	Naracauli	28	51	–	–	21	–	–	0.3	0.3
	Sa Masa	–	47	14	–	–	39	–	0.4	0.3
Roots	Unpolluted	14	–	–	–	68	–	18	0.7	0.5
	Naracauli	15	–	–	–	69	–	16	0.2	0.1
	Sa Masa	15	19	–	18	–	48	–	0.2	0.2
Stems	Unpolluted	–	–	–	16	54	–	30	0.8	0.6
	Naracauli	–	–	–	19	56	–	25	0.4	0.3
	Sa Masa	–	–	–	21	16	21	42	0.4	0.3

4. Discussion

4.1. Zinc source and complexation

Zinc plant uptake is affected by several factors such as Zn content at the soil-root interface, plant demand, and root absorption capacity (Sadeghzadeh, 2013). It remains a controversial issue whether plants predominantly absorb metal ions from soil solution (Kim et al., 2010) or from solid phases. Indeed, although the dissolved concentration in soil pore water is often used to estimate metal bioavailability, metals in minerals are key components, as plants can take up elements from the non-mobile fractions of the solids and because the solid-phase pool controls the resupply of metals to the soil solution (Hinsinger and Courchesne, 2007; Knight et al., 1997; Zhang et al., 2001). Also, metals can be taken up by plants in form of nanoparticles, through various pathways driven by the specific materials, particle morphology and size, and by the plant species, growth stage, physiological and growing conditions (Adele et al., 2018; Lv et al., 2019; Tripathi et al., 2017). The sources of Zn in the investigated systems depended on the substrate origin and the irrigation line. In the mine-waste-rich substrates, Zn primary minerals, such as hemimorphite and smithsonite, were the most abundant Zn species as revealed by XRD (Table S4) and XANES (Table 4 and Fig. S6d and h) analyses, and Zn ranged between ~10,000 and ~20,000 mg/kg. In the unpolluted substrate, Zn was mainly present as sorbed species and incorporated in layered minerals (Table 4), with a concentration of ~140 mg/kg. The detected species must be considered as dynamic Zn sources, as they are part of both biotic and abiotic bidirectional processes: from roots to the soil and from soil to the roots. Specifically, plant roots and microbial metabolism can transform metal species to facilitate metal uptake or to detoxify metals through root exudation, microorganism secretions and/or pH changes, leading to variable concentration gradients and speciation patterns, whose extent can vary through time (Adele et al., 2021; Brown et al., 1999; Kangwankraiphaisan et al., 2013; Kuzyakov and Razavi, 2019; Schnepf et al., 2022).

After five months of plant-mineral-water interaction, XRD analysis did not show any significant bulk mineralogical variation between the initial substrates and the rhizospheres for both the CW and the ZnW (Table S4), however, XANES analysis revealed that Zn supplement to the irrigation water influenced to a variable extent the Zn chemical speciation in the investigated systems. For instance, high Zn contents in water led to an increase of Zn hosted in layered minerals in the unpolluted rhizosphere (from 25 % to 48 %). Previous studies (Voegelin et al., 2005, and references therein) demonstrated that the incorporation of Zn in newly forming layered minerals (*e.g.*, LDH, phyllosilicates, or hydroxide type) may represent an important metal sequestration mechanism in soils and sediments. Our data suggest that this is an active pathway also in this study. The formation (or increase) of Zn cysteine, observed in the unpolluted rhizosphere and roots, and in Sa Masa stems from the ZnW, was probably due to *J. acutus* response to high Zn content in water. Our results support previous findings on the relevant role of cysteine in metal homeostasis, detoxification and tolerance to high concentrations of Zn in many plants, because it helps to regulate (Domínguez-Solís et al., 2004; Oven et al., 2002) and reduce the cellular bioavailability of Zn (Adediran et al., 2016; Adele et al., 2021, 2018). XANES data suggested that also citrate plays a key role in the control of Zn bioavailability, as demonstrated by its increase in the Sa Masa samples (rhizosphere and roots) from the ZnW. Indeed, citrate is a ligand involved in metal transport and storage in plants (Gramlich et al., 2013). For example, Terzano et al. (2008) found that, in the *Eruca vesicaria* edible plant, Zn accumulated outside the root endodermis with some Zn translocated in the xylem as Zn citrate. In shoots of the hyperaccumulator *Thlaspi caerulescens*, Zn citrate was the dominant species with hydrated Zn, histidine, cell wall, and oxalate playing a secondary role (Salt et al., 1999). In our experiment, the Zn supply by the water could have stimulated a higher citrate synthesis (Shen et al., 1997). The observed variations in Zn speciation for the epigean organs collected from the unpolluted and Sa Masa systems (CW *vs* ZnW) support the results reported by Da Cruz et al. (2019) that performed time resolved experiments to investigate Zn uptake, biotransformation and physiological effects on *Phaseolus vulgaris* (L.) exposed to ZnO nanoparticles (40 and 300 nm) dispersions and $ZnSO_{4(aq)}$ (Zn 100 and 1000 mg/l) for 48 h. They observed that, in leaves, Zn was mainly present as Zn phosphate (59–87 %) in all treatments, whereas Zn-histidine was detected for $ZnSO_4$, 40 and 300 nm ZnO exposures, and Zn-malate for the 300 nm treated plants, demonstrating that Zn speciation can change when the same plant species is exposed to different Zn sources.

Differently from the unpolluted and Sa Masa systems, the Naracauli system did not show any significant variation in the Zn coordination environment for the two irrigation lines. The occurrence of Zn phosphate in stems from the three systems is consistent with other studies. For instance, Zn phosphate was detected in the leaves of *Phaseolus vulgaris* (the common bean) from plants exposed to 10 mg/l Zn of $ZnSO_{4(aq)}$, and ZnO nanoparticles (40 nm and 300 nm) for seven days (da Cruz et al., 2019), and in the apoplast of tobacco roots (Straczek et al., 2008).

4.2. Plant growth and Zn accumulation

Zinc is one of the eight micronutrients (along with Mn, Cu, B, Fe, Cl, Mo and Ni) that are essential for healthy growth and reproduction of plants (Vatansever et al., 2017). It is required as a structural component of many proteins, and an insufficient amount leads to physiological stresses due to the failure of Zn dependent metabolic processes (Sadeghzadeh, 2013). On the other hand, excessive Zn (100–500 mg/kg in the vegetal organs) is toxic to plants, and leads to functional and structural disorders (Balafrej et al., 2020; Kabata-Pendias, 2000; Zeng et al., 2011). In our experiment, plant growth (Table 1 and Fig. S2) was higher for specimens grown on the unpolluted substrate (CW 29 ± 5 cm, ZnW 26 ± 1 cm), followed by the Sa Masa (CW 17.3 ± 0.9 cm, ZnW 15 ± 1 cm) and the Naracauli (CW 12 ± 1 cm, ZnW 11.8 ± 0.7 cm) substrates. This behavior could be related both to the low nutrient concentration in the Sa Masa and Naracauli substrates (Table S1, Bacchetta et al., 2015; Sprocati et al., 2014) and to the high concentration of Zn (Balafrej et al., 2020) and other metals, such as Pb (~5220–7000 mg/kg) and Cd (~19–110 mg/kg), in the mine-waste-rich substrates (Bacchetta et al., 2015; Medas et al., 2013), as *J. acutus* can tolerate exogenous Zn concentrations up to 60–100 mM (Mateos-Naranjo et al., 2014; Santos et al., 2014). Indeed, in roots and stems from the unpolluted substrate (CW and ZnW), Zn was lower than 100–500 mg/kg, thus probably not affecting the metabolic processes (Kabata-Pendias, 2000; Zeng et al., 2011), whereas in roots and stems from the polluted substrates Zn ranged between 4400 and 10,000 mg/kg and 420–1140 mg/kg, respectively. Our findings support results from Mateos-Naranjo et al. (2014) who performed a pot experiment (with perlite as growth substrate and 20 % Hoagland's solution + $ZnSO_4{\cdot}7H_2O$, Zn from 0 to 100 mM). They observed increasing Zn contents in *J. acutus* organs (up to 2500 mg/kg in roots, and up to 500 mg/kg in stems) when the plants were irrigated with solutions characterized by high Zn concentrations. In their experiment, the mean plant height was smaller in 100 mM Zn treatment than in control (Zn 0 mM). In our experiment, plant development appeared to be affected more by the composition of the substrate than by the Zn content in the water, that did not significantly affect the plant height for a specific growth substrate (Table 1 and Fig. S2).

Despite the negligible influence of the Zn content in water on plant growth, comparing samples belonging to the CW and the ZnW, some differences were observed in the Zn accumulation (Table 2 and Fig. S3) and distribution (Table 3 and Fig. S4), and they varied for the three investigated systems. The greatest variations were observed for the samples collected from the unpolluted group. Specifically, despite the increase in the Zn concentration in the unpolluted rhizosphere, roots and stems from the ZnW, the BCF, BAC and TF decreased, suggesting that a lower Zn accumulation and translocation occurred when the Zn concentration in the water was higher. This trend could be due to the incorporation of Zn in low bioavailable forms in the rhizosphere (*i.e.*, Zn-Al-

LDH in the unpolluted rhizosphere sample from the ZnW) and/or to complexation mechanisms induced by *J. acutus* to control Zn uptake (*i.e.*, Zn cysteine). On the contrary, the experiments carried out in the already polluted substrates pointed out a minor role of the Zn content in the water that had no significant effects on the Zn accumulation in stems (BAC values) and on its translocation (TF values) (Table 3 and Fig. S4).

5. Conclusions

Our rhizobox experiment explored the fate of Zn in the rhizosphere-plant system of *J. acutus*, and assessed the role played by the rhizosphere minerals and water composition on Zn uptake processes. The study highlights the complexity of the interactions among the rhizosphere, water and plants, and demonstrates that *J. acutus*, grown on different substrates, develops different complexation mechanisms when watered with Zn-spiked water. Specifically, when the unpolluted substrate is exposed to Zn flow, a partial Zn attenuation is accomplished by its incorporation in layered minerals. Plants grown on the contaminated substrates react with an exclusion strategy, *i.e.*, lower Zn translocation, to avoid detrimental effects on the plant health. Moreover, Zn tolerance is driven by changes in metal speciation, namely variation in the amount of citrate and cysteine complexes. Watering with water containing high Zn concentration did not result in similar changes in the distribution of different Zn complexes in the investigated rhizosphere-plant systems, indicating that the transformation of Zn is primarily influenced by minerals in the root zone. This aspect needs to be considered during the modeling and design of phytoremediation plans, since water composition is affected by natural seasonal variations, thus resulting in different responses of the system. Changes of bulk mineralogical composition (crystallographic phases) between rhizosphere samples from the two irrigation lines were not observed. This apparent lack of variation may be ascribed to slow reaction kinetics. Longer experimental times could lead to the formation of new crystalline phases. Their identification could be aided by the use of microanalytical techniques, such as μ-XRD mapping, instead of bulk XRD. The appearance of such new phases would have consequences for the long-term fate of Zn in these systems.

CRediT authorship contribution statement

Daniela Medas: Conceptualization, Formal analysis, Investigation, Resources, Supervision, Validation, Visualization, Writing – original draft, Writing – review & editing. **Carlo Meneghini:** Formal analysis, Funding acquisition, Investigation, Validation, Writing – original draft, Writing – review & editing. **Claudia Pusceddu:** Investigation, Methodology, Writing – review & editing. **Ilaria Carlomagno:** Formal analysis, Writing – review & editing. **Giuliana Aquilanti:** Formal analysis, Writing – review & editing. **Elisabetta Dore:** Investigation, Visualization, Writing – review & editing. **Vittorio Murgia:** Investigation, Methodology, Writing – review & editing. **Francesca Podda:** Investigation, Writing – review & editing. **Valentina Rimondi:** Investigation, Writing – review & editing. **Salvatore Vacca:** Investigation, Writing – review & editing. **Richard B. Wanty:** Investigation, Methodology, Supervision, Writing – review & editing. **Giovanni De Giudici:** Conceptualization, Funding acquisition, Methodology, Project administration, Resources, Supervision, Validation, Writing – review & editing.

Data availability

Data will be made available on request.

Declaration of competing interest

The authors declare that they have no known competing financial interests or personal relationships that could have appeared to influence the work reported in this paper.

Acknowledgments

The authors acknowledge: the CERIC-ERIC Consortium (grant number: 20167045) for the access to the XAFS beamline and financial support; the XRF beamline; CESA (E58C16000080003) from RAS, FdS (F72F16003080002, and "Sustainable land management: the tools of geology for the environment" - F75F21001270007) grants; CM acknowledges the grant Dipartimento di Eccellenza, MIUR (ARTICOLO 1, COMMI 314 e 337 LEGGE 232/2016). Finally, we would like to thank the handling Editor, Professor F.M.G. Tack, the anonymous referees for several suggestions to improve the article, and Prof. Lattanzi for his constructive suggestions during the revision of the manuscript.

Appendix A. Supplementary data

Supplementary data to this article can be found online at https://doi.org/10.1016/j.scitotenv.2023.161931.

References

Adediran, G.A., Ngwenya, B.T., Mosselmans, J.F.W., Heal, K.V., 2016. Bacteria-zinc co-localization implicates enhanced synthesis of cysteine-rich peptides in zinc detoxification when Brassica juncea is inoculated with rhizobium leguminosarum. New Phytol. 209, 280–293. https://doi.org/10.1111/nph.13588.

Adediran, G.A., Ngwenya, B.T., Mosselmans, J.F.W., Heal, K.V., Harvie, B.A., 2015. Mechanisms behind bacteria induced plant growth promotion and zn accumulation in Brassica juncea. J. Hazard. Mater. 283, 490–499. https://doi.org/10.1016/j.jhazmat.2014.09.064.

Adele, N.C., Ngwenya, B.T., Heal, K.V., Mosselmans, J.F.W., 2021. Role of plant growth promoting bacteria in driving speciation gradients across soil-rhizosphere-plant interfaces in zinc-contaminated soils. Environ. Pollut. 279, 116909. https://doi.org/10.1016/j.envpol.2021.116909.

Adele, N.C., Ngwenya, B.T., Heal, K.V., Mosselmans, J.F.W., 2018. Soil bacteria override speciation effects on zinc phytotoxicity in zinc-contaminated soils. Environ. Sci. Technol. 52, 3412–3421. https://doi.org/10.1021/acs.est.7b05094.

Alam, M.R., Rahman, M.M., Tam, N.F.-Y., Yu, R.M.K., MacFarlane, G.R., 2022. The accumulation and distribution of arsenic species and selected metals in the saltmarsh halophyte, spiny rush (Juncus acutus). Mar. Pollut. Bull. 175, 113373. https://doi.org/10.1016/j.marpolbul.2022.113373.

Ardau, C., Frau, F., Dore, E., Lattanzi, P., 2012. Molybdate sorption by Zn–Al sulphate layered double hydroxides. Appl. Clay Sci. 65–66, 128–133. https://doi.org/10.1016/j.clay.2012.05.005.

Aydın Temel, F., Avcı, E., Ardalı, Y., 2018. Full scale horizontal subsurface flow constructed wetlands to treat domestic wastewater by Juncus acutus and Cortaderia selloana. Int. J. Phytoremediat. 20, 264–273. https://doi.org/10.1080/15226514.2017.1374336.

Bacchetta, G., Cappai, G., Carucci, A., Tamburini, E., 2015. Use of native plants for the remediation of abandoned mine sites in mediterranean semiarid environments. Bull. Environ. Contam. Toxicol. 94, 326–333. https://doi.org/10.1007/s00128-015-1467-y.

Balafrej, H., Bogusz, D., Abidine Triqui, Z.-E., Guedira, A., Bendaou, N., Smouni, A., Fahr, M., 2020. Zinc hyperaccumulation in plants: a review. Plants 9, 562. https://doi.org/10.3390/plants9050562.

Bao, Z., Al, T., Bain, J., Shrimpton, H.K., Finfrock, Y.Z., Ptacek, C.J., Blowes, D.W., 2022. Sphalerite weathering and controls on zn and cd migration in mine waste rock: an integrated study from the molecular scale to the field scale. Geochim. Cosmochim. Acta 318, 1–18. https://doi.org/10.1016/j.gca.2021.11.007.

Boi, M.E., Medas, D., Aquilanti, G., Bacchetta, G., Birarda, G., Cappai, G., Carlomagno, I., Casu, M.A., Gianoncelli, A., Meneghini, C., Piredda, M., Podda, F., Porceddu, M., Rimondi, V., Vaccari, L., De Giudici, G., 2020. Mineralogy and Zn chemical speciation in a soil-plant system from a metal-extreme environment: a study on Helichrysum microphyllum subsp. tyrrhenicum (Campo Pisano Mine, SW Sardinia, Italy). Minerals 10, 259. https://doi.org/10.3390/min10030259.

Boni, M., Gilg, H.A., Aversa, G., Balassone, G., 2003. The "Calamine" of Southwest Sardinia: geology, mineralogy, and stable isotope geochemistry of supergene zn mineralization. Econ. Geol. 98, 731–748. https://doi.org/10.2113/gsecongeo.98.4.731.

Brooks, R., 2008. Plants that hyperaccumulate heavy metals. Plants and the Chemical Elements: Biochemistry, Uptake, Tolerance and Toxicity, pp. 87–105 https://doi.org/10.1002/9783527615919.ch4.

Brown, G.E., Foster, A.L., Ostergren, J.D., 1999. Mineral surfaces and bioavailability of heavy metals: a molecular-scale perspective. Proc. Natl. Acad. Sci. 96, 3388 LP–3395. https://doi.org/10.1073/pnas.96.7.3388.

Brown, K., Bettink, K., 2006. Biology of sharp rush Juncus acutus. Manangin Sharp Rush Juncus acutus. Proc. a Work. held Wollast. Coll. Conf. Cent, pp. 38–42.

Caldelas, C., Weiss, D.J., 2017. Zinc homeostasis and isotopic fractionation in plants: a review. Plant Soil 411, 17–46. https://doi.org/10.1007/s11104-016-3146-0.

Chandrakasan, G., Toledano Ayala, M., García Trejo, J.F., Marcus, G., Carroll, D.L., 2021. Mapping and distribution of speciation changes of metals from nanoparticles in environmental matrices using synchrotron radiation techniques. Environ. Nanotechnol. Monit. Manag. 16, 100491. https://doi.org/10.1016/j.enmm.2021.100491.

Chen, K.Y., Yang, P.T., Chang, H.F., Yeh, K.C., Wang, S.L., 2022. Soil gallium speciation and resulting gallium uptake by rice plants. J. Hazard. Mater. 424, 127582. https://doi.org/10.1016/j.jhazmat.2021.127582.

Christofilopoulos, S., Syranidou, E., Gkavrou, G., Manousaki, E., Kalogerakis, N., 2016. The role of halophyte Juncus acutus L. In the remediation of mixed contamination in a hydroponic greenhouse experiment. J. Chem. Technol. Biotechnol. 91, 1665–1674. https://doi.org/10.1002/jctb.4939.

Cidu, R., Biddau, R., 2005. Legacy at abandoned mines: impact of mine wastes on surface waters. Proceeding of the 9th International Mine Water Association Congress (IMWA), pp. 247–252.

Cidu, R., Frau, F., Da Pelo, S., 2011. Drainage at abandoned mine sites: natural attenuation of contaminants in different seasons. Mine Water Environ. 30, 113–126. https://doi.org/10.1007/s10230-011-0146-4.

da Cruz, T.N.M., Savassa, S.M., Montanha, G.S., Ishida, J.K., de Almeida, E., Tsai, S.M., Lavres Junior, J., Pereira de Carvalho, H.W., 2019. A new glance on root-to-shoot in vivo zinc transport and time-dependent physiological effects of ZnSO4 and ZnO nanoparticles on plants. Sci. Rep. 9, 10416. https://doi.org/10.1038/s41598-019-46796-3.

De Giudici, G., Lattanzi, P., Medas, D., 2015. Synchrotron radiation and environmental sciences. In: Mobilio, S., Boscherini, F., M.C. (Eds.), Synchrotron Radiation: Basics, Methods and Applications. Springer, Berlin Heidelberg, pp. 661–676 https://doi.org/10.1007/978-3-642-55315-8_25.

De Giudici, G., Medas, D., Cidu, R., Lattanzi, P., Rigonat, N., Frau, I., Podda, F., Marras, P.A., Dore, E., Frau, F., Rimondi, V., Runkel, R.L., Wanty, R.B., Kimball, B., 2019. Assessment of origin and fate of contaminants along mining-affected rio montevecchio (SW Sardinia, Italy): a hydrologic-tracer and environmental mineralogy study. Appl. Geochemistry 109, 104420. https://doi.org/10.1016/j.apgeochem.2019.104420.

De Giudici, G., Pusceddu, C., Medas, D., Meneghini, C., Gianoncelli, A., Rimondi, V., Podda, F., Cidu, R., Lattanzi, P., Wanty, R.B., Kimball, B.A., 2017. The role of natural biogeochemical barriers in limiting metal loading to a stream affected by mine drainage. Appl. Geochemistry 76, 124–135. https://doi.org/10.1016/j.apgeochem.2016.11.020.

de la Fuente, V., Rufo, L., Sánchez-Gavilán, I., Ramírez, E., Rodríguez, N., Amils, R., 2018. Plant tissues and embryos biominerals in Sarcocornia pruinosa, a halophyte from the Río tinto salt marshes. Minerals https://doi.org/10.3390/min8110505.

Di Cicco, A., Aquilanti, G., Minicucci, M., Principi, E., Novello, N., Cognigni, A., Olivi, L., 2009. Novel XAFS capabilities at ELETTRA synchrotron light source. J. Phys. Conf. Ser. 190, 12043. https://doi.org/10.1088/1742-6596/190/1/012043.

Domínguez-Solís, J.R., López-Martín, M.C., Ager, F.J., Ynsa, M.D., Romero, L.C., Gotor, C., 2004. Increased cysteine availability is essential for cadmium tolerance and accumulation in Arabidopsis thaliana. Plant Biotechnol. J. 2, 469–476. https://doi.org/10.1111/j.1467-7652.2004.00092.x.

Doolette, C.L., Read, T.L., Li, C., Scheckel, K.G., Donner, E., Kopittke, P.M., Schjoerring, J.K., Lombi, E., 2018. Foliar application of zinc sulphate and zinc EDTA to wheat leaves: differences in mobility, distribution, and speciation. J. Exp. Bot. 69, 4469–4481. https://doi.org/10.1093/jxb/ery236.

Dore, E., Fancello, D., Rigonat, N., Medas, D., Cidu, R., Da Pelo, S., Frau, F., Lattanzi, P., Marras, P.A., Meneghini, C., Podda, F., Rimondi, V., Runkel, R.L., Kimball, B., Wanty, R.B., De Giudici, G., 2020. Natural attenuation can lead to environmental resilience in mine environment. Appl. Geochemistry 117. https://doi.org/10.1016/j.apgeochem.2020.104597.

Duarte, B., Durante, L., Marques, J.C., Reis-Santos, P., Fonseca, V.F., Caçador, I., 2021. Development of a toxicophenomic index for trace element ecotoxicity tests using the halophyte Juncus acutus: juncus-TOX. Ecol. Indic. 121, 107097. https://doi.org/10.1016/j.ecolind.2020.107097.

Etschmann, B.E., Donner, E., Brugger, J., Howard, D.L., de Jonge, M.D., Paterson, D., Naidu, R., Scheckel, K.G., Ryan, C.G., Lombi, E., 2014. Speciation mapping of environmental samples using XANES imaging. Environ. Chem. 11, 341–350. https://doi.org/10.1071/EN13189.

Fancello, D., Scalco, J., Medas, D., Rodeghero, E., Martucci, A., Meneghini, C., De Giudici, G., 2019. XRD-thermal combined analyses: an approach to evaluate the potential of phytoremediation, phytomining, and biochar production. Int. J. Environ. Res. Public Health 16. https://doi.org/10.3390/ijerph16111976.

FAO, 2021. Standard Operating Procedure for Soil pH Determination. Rome.

Fellet, G., Marchiol, L., Perosa, D., Zerbi, G., 2007. The application of phytoremediation technology in a soil contaminated by pyrite cinders. Ecol. Eng. 31, 207–214. https://doi.org/10.1016/j.ecoleng.2007.06.011.

Fourati, E., Vogel-Mikuš, K., Wali, M., Kavčič, A., Gomilšek, J.P., Kodre, A., Kelemen, M., Vavpetič, P., Pelicon, P., Abdelly, C., Ghnaya, T., 2020. Nickel tolerance and toxicity mechanisms in the halophyte Sesuvium portulacastrum L. As revealed by ni localization and ligand environment studies. Environ. Sci. Pollut. Res. 27, 23402–23410. https://doi.org/10.1007/s11356-019-05209-8.

Frau, F., Atzori, R., Ardau, C., Medas, D., Podda, F., Dore, E., Idini, A., Tempesta, G., Agrosì, G., 2020. A two-step pH control method to remove divalent metals from near-neutral mining and metallurgical waste drainages by inducing the formation of layered double hydroxide. J. Environ. Manag. 271, 111043. https://doi.org/10.1016/j.jenvman.2020.111043.

Freitas, M., Pacheco, A.M.G., Anawar, H., Canha, N., Dionisio, I., Bettencourt, A., Henriques, F., Gomes, C., Capelo, S., 2009. Determination of phytoextraction potential of plant species for toxic elements in soils of abandoned sulphide-mining areas. J. Radioanal. Nucl. Chem. 282, 21–27. https://doi.org/10.1007/s10967-009-0222-4.

Frérot, H., Lefèbvre, C., Gruber, W., Collin, C., Santos, A.Dos, Escarré, J., 2006. Specific interactions between local metallicolous plants improve the phytostabilization of mine soils. Plant Soil 282, 53–65. https://doi.org/10.1007/s11104-005-5315-4.

Gaur, A., Shrivastava, B., 2012. A comparative study of the methods of speciation using X-ray absorption fine structure. Acta Phys. Pol. Ser. A 121, 647–652. https://doi.org/10.12693/APhysPolA.121.647.

Gramlich, A., Tandy, S., Frossard, E., Eikenberg, J., Schulin, R., 2013. Availability of zinc and the ligands citrate and histidine to wheat: does uptake of entire complexes play a Role? J. Agric. Food Chem. 61, 10409–10417. https://doi.org/10.1021/jf401117d.

Hinsinger, P., Courchesne, F., 2007. Biogeochemistry of metals and metalloids at the soil–root interface. In: Violante, A., Huang, P.M., Gadd, G.M. (Eds.), Biophysico-chemical Processes of Heavy Metals and Metalloids in Soil Environments, pp. 265–311 https://doi.org/10.1002/9780470175484.ch7.

Hylander, L.D., 2002. Improvements of rhizoboxes used for studies of soil–root interactions. Commun. Soil Sci. Plant Anal. 33, 155–161. https://doi.org/10.1081/CSS-120002384.

Jark, W., Eichert, D., Lühl, L., Gambitta, A., 2014. Optimisation of a compact optical system for the beamtransport at the X-ray fluorescence beamline at Elettra for experiments with small spots. Proc. SPIE 9207, 92070G. https://doi.org/10.1117/12.2063009.

Kabata-Pendias, A., 2000. Trace Elements in Soils and Plants. CRC Press, Boca Raton, FL, Boca Raton.

Kangwankraiphaisan, T., Suntornvongsagul, K., Sihanonth, P., Klysubun, W., Gadd, G., 2013. Influence of arbuscular mycorrhizal fungi (AMF) on zinc biogeochemistry in the rhizosphere of Lindenbergia philippensis growing in zinc-contaminated sediment. Biometals 26, 489–505. https://doi.org/10.1007/s10534-013-9634-2.

Kim, K.R., Owens, G., Naidu, R., 2010. Effect of root-induced chemical changes on dynamics and plant uptake of heavy metals in rhizosphere soils. Pedosphere 20, 494–504. https://doi.org/10.1016/S1002-0160(10)60039-2.

Knight, B., Zhao, F.J., McGrath, S.P., Shen, Z.G., 1997. Zinc and cadmium uptake by the hyperaccumulator Thlaspi caerulescens in contaminated soils and its effects on the concentration and chemical speciation of metals in soil solution. Plant Soil 197, 71–78. https://doi.org/10.1023/A:1004255323909.

Kopittke, P.M., Wang, P., Lombi, E., Donner, E., 2017. Synchrotron-based X-ray approaches for examining toxic trace metal(loid)s in soil-plant systems. J. Environ. Qual. 46, 1175–1189. https://doi.org/10.2134/jeq2016.09.0361.

Kothe, E., Büchel, G., 2014. UMBRELLA: using MicroBes for the REgulation of heavy metaL mobiLity at ecosystem and landscape scAle. Environ. Sci. Pollut. Res. 21, 6761–6764. https://doi.org/10.1007/s11356-014-2689-y.

Kuzyakov, Y., Razavi, B.S., 2019. Rhizosphere size and shape: temporal dynamics and spatial stationarity. Soil Biol. Biochem. 135, 343–360. https://doi.org/10.1016/j.soilbio.2019.05.011.

Kwon, M.J., Boyanov, M.I., Mishra, B., Kemner, K.M., Jeon, S., Hong, J.K., Lee, S., 2022. Zn speciation and fate in soils and sediments along the ground transportation route of Zn ore to a smelter. J. Hazard. Mater. 129422. https://doi.org/10.1016/j.jhazmat.2022.129422.

Landsberger, S., Robinson, S., Freitas, M., Canha, N., Pacheco, A., Anawar, H., 2010. Characterisation of antimony, arsenic, cadmium, copper and tin occurrences at an abandoned sulphide-mining area. Int. J. Environ. Heal. 4, 166–180. https://doi.org/10.1504/IJENVH.2010.033706.

Lombardo, A., 1982. Flora montevidensis. Intendencia municipal de Montevideo. Flora Montevidensis. Intend. Munic. Montevideo 1, 366–367.

López-Juambeltz, F., Rodríguez-Gallego, L., Dabezíes, J.M., Chreties, C., Narbondo, S., Conde, D., 2020. A GIS-based assessment combined with local ecological knowledge to support the management of Juncus acutus L. spreading in the floodplain of a protected coastal lagoon. J. Nat. Conserv. 57, 125891. https://doi.org/10.1016/j.jnc.2020.125891.

Lv, J., Christie, P., Zhang, S., 2019. Uptake, translocation, and transformation of metal-based nanoparticles in plants: recent advances and methodological challenges. Environ. Sci. Nano 6, 41–59. https://doi.org/10.1039/C8EN00645H.

Marchand, L., Mench, M., Jacob, D.L., Otte, M.L., 2010. Metal and metalloid removal in constructed wetlands, with emphasis on the importance of plants and standardized measurements: a review. Environ. Pollut. 158, 3447–3461. https://doi.org/10.1016/j.envpol.2010.08.018.

Marchiol, L., Felle, T.G., Boscutti, F., Montella, C., Mozzi, R., Guarino, C., 2013. Gentle remediation at the former "Pertusola Sud" zinc smelter: evaluation of native species for phytoremediation purposes. Ecol. Eng. 53, 343–353. https://doi.org/10.1016/j.ecoleng.2012.12.072.

Mateos-Naranjo, E., Castellanos, E.M., Perez-Martin, A., 2014. Zinc tolerance and accumulation in the halophytic species Juncus acutus. Environ. Exp. Bot. 100, 114–121. https://doi.org/10.1016/j.envexpbot.2013.12.023.

Mateos-Naranjo, E., Pérez-Romero, J.A., Redondo-Gómez, S., Mesa-Marín, J., Castellanos, E.M., Davy, A.J., 2018. Salinity alleviates zinc toxicity in the saltmarsh zinc-accumulator Juncus acutus. Ecotoxicol. Environ. Saf. 163, 478–485. https://doi.org/10.1016/j.ecoenv.2018.07.092.

Medas, D., Carlomagno, I., Meneghini, C., Aquilanti, G., Araki, T., Bedolla, D.E., Buosi, C., Casu, M.A., Gianoncelli, A., Kuncser, A.C., Maraloiu, V.A., Giudici, G.De, 2018. Zinc incorporation in marine bivalve shells grown in mine-polluted seabed sediments : a case study in the Malfidano mining area (SW Sardinia, Italy). Environ. Sci. Pollut. Res. https://doi.org/10.1007/s11356-018-3504-y.

Medas, D., Cidu, R., De Giudici, G., Podda, F., 2013. Geochemistry of rare earth elements in water and solid materials at abandoned mines in SW Sardinia (Italy). J. Geochem. Explor. 133. https://doi.org/10.1016/j.gexplo.2013.05.005.

Medas, D., Cidu, R., Lattanzi, P., Podda, F., Wanty, R.B., De Giudici, G., 2012. Hydrozincite seasonal precipitation at naracauli (Sardinia - Italy): hydrochemical factors and morphological features of the biomineralization process. Appl. Geochem. 27. https://doi.org/10.1016/j.apgeochem.2012.02.016.

Medas, D., De Giudici, G., Pusceddu, C., Casu, M.A., Birarda, G., Vaccari, L., Gianoncelli, A., Meneghini, C., 2019. Impact of zn excess on biomineralization processes in Juncus acutus grown in mine polluted sites. J. Hazard. Mater. 370, 98–107. https://doi.org/10.1016/j.jhazmat.2017.08.031.

Montanha, G.S., Rodrigues, E.S., Romeu, S.L.Z., de Almeida, E., Reis, A.R., Lavres, J., Pereira de Carvalho, H.W., 2020. Zinc uptake from ZnSO4 (aq) and Zn-EDTA (aq) and its root-to-shoot transport in soybean plants (Glycine max) probed by time-resolved in vivo X-ray spectroscopy. Plant Sci. 292, 110370. https://doi.org/10.1016/j.plantsci.2019.110370.

Oven, M., Grill, E., Golan-Goldhirsh, A., Kutchan, T.M., Zenk, M.H., 2002. Increase of free cysteine and citric acid in plant cells exposed to cobalt ions. Phytochemistry 60, 467–474. https://doi.org/10.1016/S0031-9422(02)00135-8.

Panfili, F., Manceau, A., Sarret, G., Spadini, L., Kirpichtchikova, T., Bert, V., Laboudigue, A., Marcus, M.A., Ahamdach, N., Libert, M.-F., 2005. The effect of phytostabilization on zn speciation in a dredged contaminated sediment using scanning electron microscopy, X-ray fluorescence, EXAFS spectroscopy, and principal components analysis. Geochim. Cosmochim. Acta 69, 2265–2284. https://doi.org/10.1016/j.gca.2004.10.017.

Parsons, J.G., Aldrich, M.V., Gardea-Torresdey, J.L., 2002. Environmental and biological applications of extended X-ray absorption fine structure (EXAFS) and X-ray absorption near edge structure (XANES) spectroscopies. Appl. Spectrosc. Rev. 37, 187–222. https://doi.org/10.1081/ASR-120006044.

Pavoni, E., Covelli, S., Adami, G., Baracchini, E., Cattelan, R., Crosera, M., Higueras, P., Lenaz, D., Petranich, E., 2018. Mobility and fate of thallium and other potentially harmful elements in drainage waters from a decommissioned Zn-Pb mine (North-eastern Italian Alps). J. Geochem. Explor. 188, 1–10. https://doi.org/10.1016/j.gexplo.2018.01.005.

Pérez-Esteban, J., Escolástico, C., Moliner, A., Masaguer, A., Ruiz-Fernández, J., 2014. Phytostabilization of metals in mine soils using Brassica juncea in combination with organic amendments. Plant Soil 377, 97–109. https://doi.org/10.1007/s11104-013-1629-9.

Ravel, B., Newville, M., 2005. ATHENA, ARTEMIS, HEPHAESTUS: data analysis for X-ray absorption spectroscopy using IFEFFIT. J. Synchrotron Radiat. 12, 537–541. https://doi.org/10.1107/S0909049505012719.

Sadeghzadeh, B., 2013. A review of zinc nutrition and plant breeding. J. Soil Sci. Plant Nutr. 13, 905–927. https://doi.org/10.4067/S0718-95162013005000072.

Salt, D.E., Blaylock, M., Kumar, N.P.B.A., Dushenkov, V., Ensley, B.D., Chet, I., Raskin, I., 1995. Phytoremediation: a novel strategy for the removal of toxic metals from the environment using plants. Bio/Technology 13, 468–474. https://doi.org/10.1038/nbt0595-468.

Salt, D.E., Prince, R.C., Baker, A.J.M., Raskin, I., Pickering, I.J., 1999. Zinc ligands in the metal hyperaccumulator Thlaspi caerulescens as determined using X-ray absorption spectroscopy. Environ. Sci. Technol. 33, 713–717. https://doi.org/10.1021/es980825x.

Santos, D., Duarte, B., Caçador, I., 2014. Unveiling zn hyperaccumulation in Juncus acutus: implications on the electronic energy fluxes and on oxidative stress with emphasis on non-functional zn-chlorophylls. J. Photochem. Photobiol. B Biol. 140, 228–239. https://doi.org/10.1016/j.jphotobiol.2014.07.019.

Saraswat, S., Rai, J.P.N., 2011. Complexation and detoxification of Zn and Cd in metal accumulating plants. Rev. Environ. Sci. BioTechnol. 10, 327–339. https://doi.org/10.1007/s11157-011-9250-y.

Sarret, G., Harada, E., Choi, Y.E., Isaure, M.P., Geoffroy, N., Fakra, S., Marcus, M.A., Birschwilks, M., Clemens, S., Manceau, A., 2006. Trichomes of tobacco excrete zinc as zinc-substituted calcium carbonate and other zinc-containing compounds. Plant Physiol. 141, 1021–1034. https://doi.org/10.1104/pp.106.082743.

Sarret, G., Saumitou-Laprade, P., Bert, V., Proux, O., Hazemann, J.-L., Traverse, A., Marcus, M.A., Manceau, A., 2002. Forms of zinc accumulated in the hyperaccumulator Arabidopsis halleri. Plant Physiol. 130, 1815 LP–1826. https://doi.org/10.1104/pp.007799.

Sarret, G., Smits, E.A.H.P., Michel, H.C., Isaure, M.P., Zhao, F.J., Tappero, R., 2013. Chapter one - use of synchrotron-based techniques to elucidate metal uptake and metabolism in plants. in AIn: Sparks, D.L.B.T.-A. (Ed.), Advances in Agronomy. Academic Press, pp. 1–82 https://doi.org/10.1016/B978-0-12-407247-3.00001-9.

Schnepf, A., Carminati, A., Ahmed, M.A., Ani, M., Benard, P., Bentz, J., Bonkowski, M., Knott, M., Diehl, D., Duddek, P., Kröner, E., Javaux, M., Landl, M., Lehndorff, E., Lippold, E., Lieu, A., Mueller, C.W., Oburger, E., Otten, W., Portell, X., Phalempin, M., Prechtel, A., Schulz, R., Vanderborght, J., Vetterlein, D., 2022. Linking rhizosphere processes across scales: opinion. Plant Soil https://doi.org/10.1007/s11104-022-05306-7.

Shen, Z.G., Zhao, F.J., McGrath, S.P., 1997. Uptake and transport of zinc in the hyperaccumulator Thlaspi caerulescens and the non-hyperaccumulator Thlaspi ochroleucum. Plant Cell Environ. 20, 898–906. https://doi.org/10.1046/j.1365-3040.1997.d01-134.x.

Shi, J., Wu, B., Yuan, X., YY, C., Chen, X., Chen, Y., Hu, T., 2008. An X-ray absorption spectroscopy investigation of speciation and biotransformation of copper in Elsholtzia splendens. Plant Soil 302, 163–174. https://doi.org/10.1007/s11104-007-9463-6.

Sparks, E.L., Cebrian, J., Biber, P.D., Sheehan, K.L., Tobias, C.R., 2013. Cost-effectiveness of two small-scale salt marsh restoration designs. Ecol. Eng. 53, 250–256. https://doi.org/10.1016/j.ecoleng.2012.12.053.

Sprocati, A.R., Alisi, C., Pinto, V., Montereali, M.R., Marconi, P., Tasso, F., Turnau, K., De Giudici, G., Goralska, K., Bevilacqua, M., Marini, F., Cremisini, C., 2014. Assessment of the applicability of a "toolbox" designed for microbially assisted phytoremediation: the case study at ingurtosu mining site (Italy). Environ. Sci. Pollut. Res. 21, 6939–6951. https://doi.org/10.1007/s11356-013-2154-3.

Stefani, A., Arduini, I., Onnis, A., 1991. Juncus acutus: germination and initial growth in presence of heavy metals. Ann. Bot. Fenn. 28, 37–43.

Straczek, A., Sarret, G., Manceau, A., Hinsinger, P., Geoffroy, N., Jaillard, B., 2008. Zinc distribution and speciation in roots of various genotypes of tobacco exposed to zn. Environ. Exp. Bot. 63, 80–90. https://doi.org/10.1016/j.envexpbot.2007.10.034.

Syranidou, E., Christofilopoulos, S., Gkavrou, G., Thijs, S., Weyens, N., Vangronsveld, J., Kalogerakis, N., 2016. Exploitation of endophytic bacteria to enhance the phytoremediation potential of the wetland helophyte Juncus acutus. Front. Microbiol. 7, 1016. https://doi.org/10.3389/fmicb.2016.01016.

Syranidou, E., Christofilopoulos, S., Kalogerakis, N., 2017a. Juncus spp.—The helophyte for all (phyto)remediation purposes? New Biotechnol. 38, 43–55. https://doi.org/10.1016/j.nbt.2016.12.005.

Syranidou, E., Christofilopoulos, S., Politi, M., Weyens, N., Venieri, D., Vangronsveld, J., Kalogerakis, N., 2017b. Bisphenol-a removal by the halophyte Juncus acutus in a phytoremediation pilot: characterization and potential role of the endophytic community. J. Hazard. Mater. 323, 350–358. https://doi.org/10.1016/j.jhazmat.2016.05.034.

Terzano, R., Al Chami, Z., Vekemans, B., Janssens, K., Miano, T., Ruggiero, P., 2008. Zinc distribution and speciation within rocket plants (Eruca vesicaria L. Cavalieri) grown on a polluted soil amended with compost as determined by XRF microtomography and micro-XANES. J. Agric. Food Chem. 56, 3222–3231. https://doi.org/10.1021/jf073304e.

Tripathi, D.K., Shweta, Singh, Shweta, Singh, Swati, Pandey, R., Singh, V.P., Sharma, N.C., Prasad, S.M., Dubey, N.K., Chauhan, D.K., 2017. An overview on manufactured nanoparticles in plants: Uptake, translocation, accumulation and phytotoxicity. Plant Physiol. Biochem 110, 2–12. https://doi.org/10.1016/j.plaphy.2016.07.030.

Vatansever, R., Ozyigit, I.I., Filiz, E., 2017. Essential and beneficial trace elements in plants, and their transport in roots: a review. Appl. Biochem. Biotechnol. 181, 464–482. https://doi.org/10.1007/s12010-016-2224-3.

Voegelin, A., Pfister, S., Scheinost, A.C., Marcus, M.A., Kretzschmar, R., 2005. Changes in zinc speciation in field soil after contamination with zinc oxide. Environ. Sci. Technol. 39, 6616–6623. https://doi.org/10.1021/es047962g.

Wang, L., Rinklebe, J., Tack, F.M.G., Hou, D., 2021. A review of green remediation strategies for heavy metal contaminated soil. Soil Use Manag. 37, 936–963. https://doi.org/10.1111/sum.12717.

Wang, P., Menzies, N.W., Lombi, E., McKenna, B.A., Johannessen, B., Glover, C.J., Kappen, P., Kopittke, P.M., 2013. Fate of ZnO nanoparticles in soils and cowpea (Vigna unguiculata). Environ. Sci. Technol. 47, 13822–13830. https://doi.org/10.1021/es403466p.

Webb, S.M., 2005. SIXpack: a graphical user interface for XAS analysis using IFEFFIT. Phys. Scr. T T115, 1011–1014. https://doi.org/10.1238/Physica.Topical.115a01011.

Zaimoglu, Z., 2006. Treatment of campus wastewater by a pilot-scale constructed wetland utilizing Typha latifolia, Juncus acutus and Iris versicolor. J. Environ. Biol. 27, 293–298.

Zelano, I.O., Cloquet, C., van der Ent, A., Echevarria, G., Gley, R., Landrot, G., Pollastri, S., Fraysse, F., Montargès-Pelletier, E., 2020. Coupling nickel chemical speciation and isotope ratios to decipher nickel dynamics in the Rinorea cf. Bengalensis -soil system in malaysian Borneo. Plant Soil 454, 225–243. https://doi.org/10.1007/s11104-020-04541-0.

Zeng, X.-W., Ma, L.Q., Qiu, R.-L., Tang, Y.-T., 2011. Effects of zn on plant tolerance and non-protein thiol accumulation in zn hyperaccumulator Arabis paniculata franch. Environ. Exp. Bot. 70, 227–232. https://doi.org/10.1016/j.envexpbot.2010.09.009.

Zhang, H., Zhao, F.-J., Sun, B., Davison, W., Mcgrath, S.P., 2001. A new method to measure effective soil solution concentration predicts copper availability to plants. Environ. Sci. Technol. 35, 2602–2607. https://doi.org/10.1021/es000268q.

Zhao, F.-J., Moore, K.L., Lombi, E., Zhu, Y.-G., 2014. Imaging element distribution and speciation in plant cells. Trends Plant Sci. 19, 183–192. https://doi.org/10.1016/j.tplants.2013.12.001.

Zhou, L., Meng, Y., Vaghefi, S.A., Marras, P.A., Sui, C., Lu, C., Abbaspour, K.C., 2020. Uncertainty-based metal budget assessment at the watershed scale: implications for environmental management practices. J. Hydrol. 584. https://doi.org/10.1016/j.jhydrol.2020.124699.

Zoumis, T., Calmano, W., Förstner, U., 2000. Demobilization of heavy metals from mine waters. Acta Hydrochim. Hydrobiol. 28, 212–218. https://doi.org/10.1002/1521-401X(20004)28:4<212::AID-AHEH212>3.0.CO;2-U.

Zovko, M., Romic, M., 2011. Soil contamination by trace metals: geochemical behaviour as an element of risk assessment. In: Dar, I.A. (Ed.), Earth and Environmental Sciences. InTech, pp. 437–456 https://doi.org/10.5772/25448.